

High-Brightness linac for the Advanced Free-Electron Laser Initiative at Los Alamos\*

R. L. Sheffield, B. E. Carlsten, and L. M. Young  
 Los Alamos National Laboratory  
 Los Alamos, NM 87545

Abstract

This paper describes the design of an accelerator that can produce beams of greater than  $1 \times 10^{13}$  A/m<sup>2</sup> (brightness =  $2 \cdot I / \epsilon^2$ , where  $\epsilon$  is the rms emittance). The beam emittance growth in the accelerator is minimized by: producing a short-electron bunch in a high-gradient rf cavity, using a focusing solenoid to correct the emittance growth caused by space charge, and designing the coupling slots between accelerator cavities to minimize quadrupole effects. The results from simulations are, at 2.3 nC, a peak current of 180 A and an emittance of  $1.6 \pi$  mm-mrad, and, at 4.6 nC a peak current of 300 A and an emittance of  $2.4 \pi$  mm-mrad. The exit energy from the linac is 20 MeV for both cases.

Introduction

A new accelerator design that produces a very bright electron beam in a compact form has been developed through the Advanced Free-Electron Laser Initiative (AFELI) [1] at Los Alamos National Laboratory. State-of-the-art components will be incorporated so that the FEL system will be compact, robust, and user friendly.

The following definition is used for the normalized rms emittance,

$$\epsilon_n = \beta \gamma \epsilon_x = \pi \beta \gamma [\langle x^2 \rangle \langle x'^2 \rangle - \langle x \cdot x' \rangle^2]^{1/2},$$

where  $\gamma$  is the relativistic factor,  $\beta$  is the particle velocity divided by the speed of light,  $x$  is the transverse beam size,  $x'$  is the transverse beam divergence, and  $\epsilon_x$  is the unnormalized emittance. The emittance is calculated in two ways. The "full" emittance is calculated by using the entire micropulse in time and space. The "slice" emittance is calculated by dividing a micropulse into slices in time equal to a slippage length. To ensure enough particles are in a slice to give reasonable statistics, the smallest time slice is limited to 1% of the total pulse length. We calculate the slice emittance because the electrons do not generate gain over the entire pulse, but only for the middle portion (in time) of the pulse. If temporal mixing occurs, the use of slice emittance is invalid and the full rms emittance must be used.

Overall Accelerator Design

The design goals for the accelerator is  $> 2$  nC charge per micropulse and an effective emittance of less than  $3 \pi$  mm-mrad. Simple design is accomplished by using a single radio-frequency feed to drive the entire accelerator structure. The accelerator (Fig. 1) design has the following features: 20-MeV output energy, average cavity gradients of 22 MeV/m, up to 20-Hz repetition rate, up to 50-ms long macropulses, 8- to 20-ps long micropulses, and liquid-nitrogen operation. The accelerator operates with a 1300-MHz, 20-MW-peak-power klystron.[1]

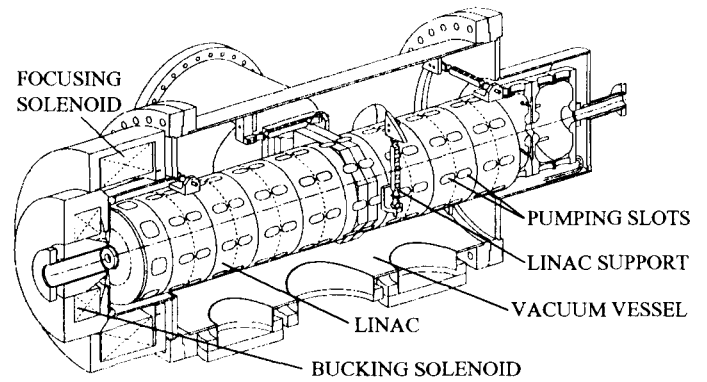


Figure 1. AFEL linac schematic.

Using a Solenoid to Compensate for Emittance Growth Caused by Space Charge

The use of a solenoid to reduce emittance growth caused by space charge has been discussed in several papers.[2] A representative configuration is shown in Fig. 2. At the cathode, the electron bunch emittance is determined by the cathode's thermal emittance (position 1 in Fig. 2). As an electron bunch leaves the cathode, the bunch expands radially because of radial space charge forces. Since the space charge force acts continuously on the bunch, no single discrete lens can compensate for the distortion of the distribution in phase space (position 2 in Fig. 2). However, a simple lens can be used to focus the bunch (position 3 in Fig. 2). Then, to the first order, the same forces that acted on the bunch during expansion are present while the bunch is focused (position 4 in Fig. 2). Thus, the emittance growth that has occurred can be significantly reduced by proper lens placement. A unique solenoid design follows from the

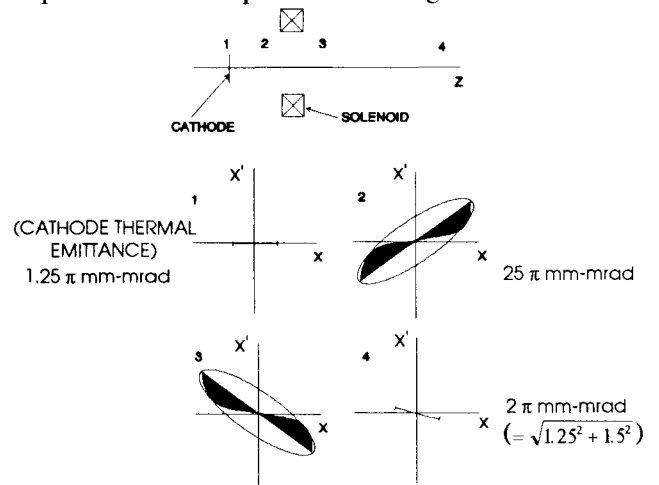


Figure 2. Placing a solenoid near the cathode can compensate for space-charge emittance growth. Position 1 is at the cathode. Position's 2 and 3 are before and after the solenoid center (with the center between 5 and 15 cm from the cathode). Position 4 is downstream of the accelerator. The figure also shows the growth in emittance ( $1.5 \pi$  mm-mrad) above the thermal emittance ( $1.25 \pi$  mm-mrad) present at the cathode.

\*Work supported by Los Alamos National Laboratory Institutional Supporting Research, under the auspices of the United States Department of Energy.

requirements of minimum emittance growth and simultaneously having the beam focused at a particular axial location. The solenoid design depends on the accelerator gradient, current density, and location of the peak magnetic field with respect to the cathode. The emittance numbers in Fig. 2 are from a typical PARMELA run. To accurately render the solenoid field profiles, we incorporated the POISSON field maps of the solenoid directly into a modified version PARMELA.

From simulations, we computed the effect on the final emittance caused from the cathode thermal effects. As expected, the final emittance is the sum of squares of the final emittance calculated with zero cathode temperature and the finite cathode emittance. An example is shown in Fig. 2.

### Minimizing Perturbations caused by Accelerator Coupling Slots

The standing-wave, 1300-MHz,  $\pi$ -mode accelerator is designed with on-axis coupling slots. By incorporating MAFIA field maps of the coupling slots into PARMELA, we found that the coupling slots produced a quadrupole lens in every accelerator cell. Therefore, it was necessary to change the coupling slot geometries to eliminate asymmetric focusing in the accelerator.

Several possible types of on-axis coupling are shown in Fig. 2. The effect of coupling slots is significant for very high-brightness beams. A single slot produces a dipole lens, two slots produce a quadrupole lens, four slots produces an octupole lens, and so on. Each accelerator cell (except the cells at the accelerator ends) has coupling slots on each half of an accelerator cell. The relative orientation of the slots on either end of the cell will determine the relative angle of the corresponding lens. The two-coupling-slot configuration gives a quadrupole lens at the entrance and exit of the accelerator cell. The orientation of the slots will determine whether the quadrupole lens add or subtract focusing for each cell. In the first arrangement, type T, the fields at each cell end cancel, giving a net effect close to zero only for a highly relativistic beam. In type H, the fields at each cell end are additive, giving a net quadrupole lens. PARMELA simulations show a very unsymmetrical beam at the exit of the accelerator for an accelerator with all type T for type H cells.

The coupling-slot design for the AFEL accelerator uses a four-coupling-slot arrangement for the first two cells and a type T configuration for the remaining accelerator cells. Because the four-slot arrangement has no quadrupole component, then the first two cells produce no beam asymmetry. After the beam exits the first two cells, the beam is highly relativistic and the type T coupling gives a very small net quadrupole focusing.

The four-coupling-slot arrangement cannot be carried throughout the accelerator. At the high-average currents of the AFEL, beam breakup will occur because of the coupling of a dipole mode from cell to cell. In the type T- and H-coupling-cell configuration, the dipole mode does not couple because the coupling slots are rotated 90° in the coupling cavity. In the 4-slot coupling-cells, the slots are rotated 45° in the coupling cavity, which very effectively couples the dipole modes.

### Other Features of the AFEL Accelerator

The first cell, a half-cell, is 9 mm longer than one-half of a standard 1300-Mhz cell. A longer injection cell has two advantages. First, the exit phase of the electron bunch depends on the cell length. Since the AFEL linac has a single rf feed, the

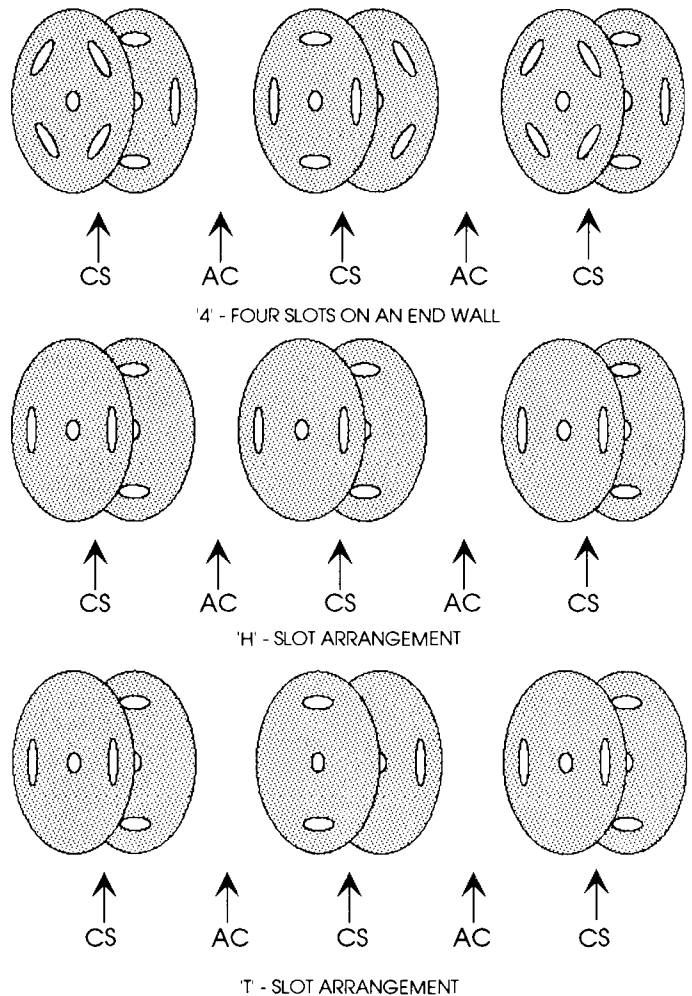


Figure 3. Possible coupling-slot arrangements with four- and two-slot coupling. CS is a coupling cell. AC is an accelerator cell.

proper operating phase to minimize energy spread was met by adjusting the first cell length. If the minimum energy spread is outside the phase tuning range, a passive cavity following the linac will be used to minimize energy spread. Second, a longer first cell increases the electron-beam energy at the exit of the first cell. This reduces the space-charge effects and helps improve the final emittance. The exit energy from the first cell is 1.5 MeV instead of 1.0 MeV for a regular half-cell.

Other engineering features of the AFEL accelerator are the capability of operation at 77K; UHV design; and high-Q, high-gradient, long-macropulse accelerator cells.

### Beam Dependencies

This type of accelerator is unique in that the electron-beam distribution does not mix longitudinally. With no mixing, the rms emittance calculation for the full pulse underestimates the FEL performance. Except for statistical noise caused by the limited number of particles in the simulation, the slice emittance is time independent during the micropulse. However, the emittance of the full pulse is significantly larger. The larger full-pulse emittance is caused from the variation in divergence throughout the micropulse (see top graph in Fig. 4). Two factors help determine FEL performance: first, the local beam conditions

in the micropulse (since the slippage length is a small fraction of the entire pulse length); second, the ability to match into the gain profile of the wiggler. Figure 4 shows the beam conditions that affect FEL performance. The upper two graphs are the beam divergence and the particle density as a function of time. The lower graph is a calculation of  $\Delta v$  (gain width [3]) for a sample wiggler) as a function of time. The three graphs show that most of the electrons are in the gain width of the wiggler for the middle portion of a micropulse. The beginning and end of the micropulse are not matched into the wiggler, but the fraction of the electrons in the temporal wings is small. Again, this type of analysis is not correct if the beam mixes longitudinally.

The AFEL is designed to minimize components and distances and to increase reliability and ease of use. However, the performance of the FEL design does depend strongly on a few parameters. The parameters that must be tightly controlled are the radius of the cathode; the magnitude of the solenoid field around the cathode region; the accelerator phase; and the magnitude of the accelerator fields.

### Results

The following results are based on the performance of the FEL using the slice emittance as opposed to the integrated emittance of the entire micropulse. This implies that the contribution of the temporal tails of the micropulse is ignored. The results are:

- The largest component of the emittance is caused by the variation of the radial velocity during the micropulse and is correlated.
- The next largest component of the emittance is caused by radial rf effects.
- A Gaussian pulse in time gives almost the same performance as a square pulse in time.
- A micropulse of 2.3 nC has a slice emittance less than  $1.5 \pi$  mm-mrad, a peak current greater than 175 A, and an effective energy spread of less than 0.3%.
- A micropulse of 4.6 nC has a slice emittance less than  $2.5 \pi$  mm-mrad, a peak current greater than 310 A, and an effective energy spread of less than 0.3%.

Simulations show that visible wavelength operation (>50% gain @ 400 nm) is possible using a low-energy (20 MeV), high-gradient (>20 MeV/m) accelerator.

### References

- [1] K. C. D. Chan,, R. H. Kraus, J. Ledford, K.L. Meier, R. E. Meyer, D. Nguyen, R. L. Sheffield, F. E. Sigler, L. M. Young, T. S. Wang, W. L. Wilson, and R. L. Wood, Nucl. Inst. Meth. in Phys., **A318**, 148 (1992).
- [2] B. E. Carlsten, Proc.10th Int. FEL Conf., Jerusalem, Israel, 1988, Nucl. Instr. and Meth., A285 (1989) 313; B. E. Carlsten and R. L. Sheffield, Poc. 1988 Linac Conf., Williamsburg, Va, 1988, CEBAF Report 89-001 (1989) 365; B. E. Carlsten, Poc. 1989 IEEE Part. Accel. Conf., Chicago, IL, IEEE Catalog no. 89CH2669-0 (1989) 313.
- [3] W. B. Colson, G. Dattoli, and F. Ciocci, *Phys Rev. A*, **64**, 2 (1985).

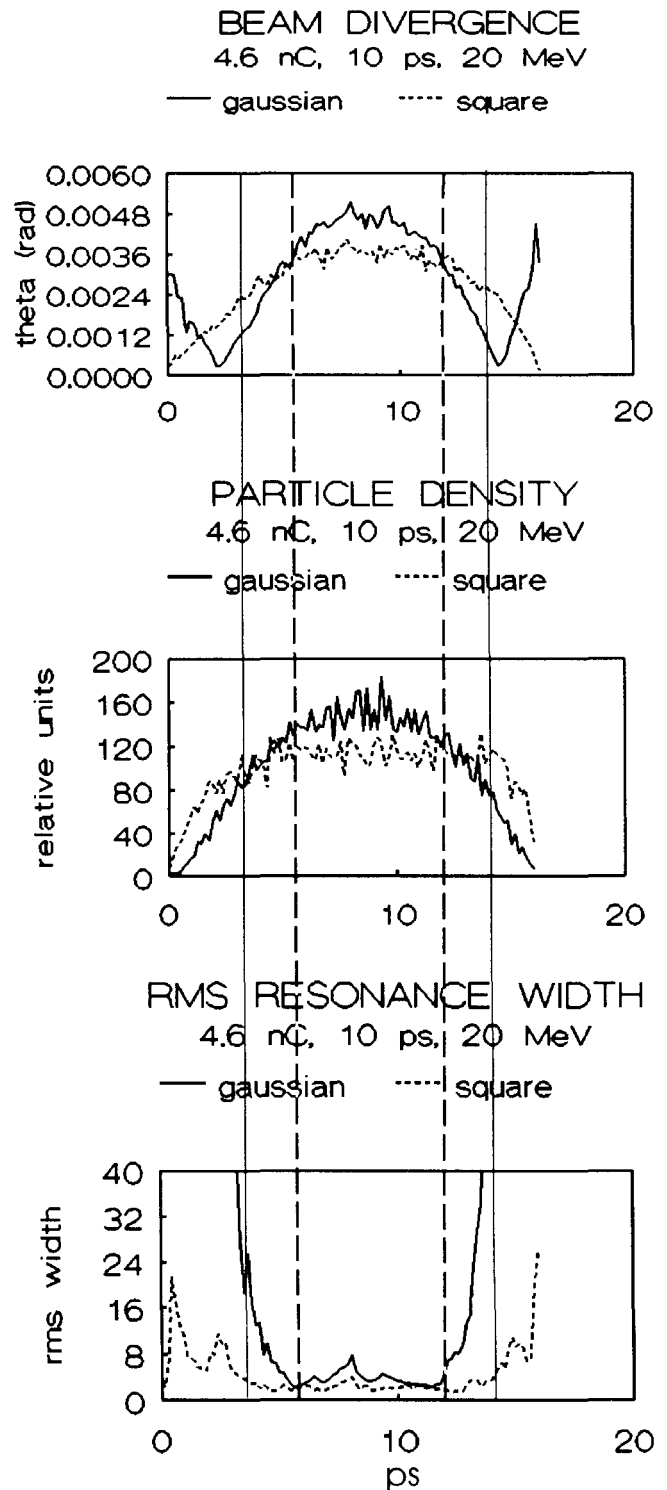


Figure 4. The upper plot shows the beam divergence during the pulse. The middle plot shows the charge density during the pulse. The bottom plot shows how well matched the pulse is to the gain profile of the wiggler.